JOURNAL OF MATERIALS SCIENCE **38** (2003) 597–601

A Raman study into the effect of transcrystallisation on thermal stresses in embedded single fibres

A. S. NIELSEN, R. PYRZ*
Institute of Mechanical Engineering, Aalborg University, Pontopidanstraede 101, 9220 Aalborg, Denmark
E-mail: rp@ime.auc.dk

Thermal stresses have been measured in single carbon fibre polypropylene matrix composites using micro Raman spectroscopy. The study focuses on the influence of a transcrystalline interlayer on the thermal residual stress distribution in composites. A series of three experiments were made in order to systematically study the influence of thermal history, transcrystalline interlayer thickness and matrix supermolecular structure. From the experiments it was shown that the transcrystalline interlayer results in higher thermal residual shear stress. This was explained by anisotropy in the transcrystalline interlayer resulting in higher radial thermal expansion and thus higher radial stress.

1. Introduction

Thermal stresses in a fibre reinforced composite are determined by the interaction between the solidifying matrix and the fibre. In composites with a semicrystalline matrix solidification isassociated with crystallisation. In semicrystalline thermoplastic matrix composites transcrystallisation often takes place. Transcrystallisation occurs when spherulites are heterogeneously nucleated on the fibre surface. As the spherulites impinge theygrow radially from the fibre forming the transcrystalline interlayer. This phenomenon has been observed in several commercial semicrystalline matrices such as polyetheretherketone, polypropylene, polyethylene, polyphenylenesulphide and polyamide [1–18]. Factors that may influence the heterogeneous nucleation are the surface energy of substrate, adsorption of molecular entities, epitaxity, melt time and temperature, cooling rate and flow field [1, 2, 19]. Experimental studies on single fibre polypropylene (PP) matrix composites have shown that transcrystallisation increases the efficiency of stress transfer at the fibre-matrix interface [20–22]. Consequently the presence of a transcrystalline interlayer affects the thermal stresses as well as the redistribution of stresses during subsequent mechanical loading. However the mechanisms governing this increased stress transfer in the presence of the transcrystalline interlayer have not yet been clarified. In composites with apolar matrices such as PP stress transfer is of a frictional nature governed by secondary van der Waals bonds [24, 25]. In such systems stress transfer may be described in terms of a Coulomb frictional type where the coefficient of "friction" relates to physiochemical interactions at the interface. An enhanced stress transfer due to transcrystallinity may then be due to an increased coefficient of "friction" as a result of the heterogeneous nucleation or due to increased residual compressive stresses at the interface due to anisotropy of the transcrystalline interlayer.

This paper describes a systematic study into the effect of transcrystallisation on the thermal stresses in composites. The experimental study utilises Raman spectroscopy. Using this technique it is possible to measure thermal stress distribution pointwise within embedded single fibres and thus to determine the interfacial shear stress distribution. The purpose of the study is to provide further experimental evidence of the mechanisms governing stress transfer in the presence of a transcrystalline interlayer.

2. Experimental

2.1. Materials and sample preparation

Two grades of isotactic polypropylene were used as matrix. These differed only by their rheological behaviour with melt flow indices (MFI) of 14 (PPa) and 5.5 (PPb). Single fibre composites were prepared by placing a fibre, approximately 1 mm in length, between two polymer films of 80–100 μm in thickness (Fig. 1). The fibre used was a PAN based high modulus carbon fibre (350 GPa). The fibre was thoroughly cleaned to remove any sizing and subsequently dried under vacuum.

The assembly was placed on a thin glass slide covered with a thin layer of silicon oil and placed in a Linkam THMS600 thermal stage. The sample was melted at 205°C for 5 min. The influence of heat transfer from

*Author to whom all correspondance should be addressed.

TABLE I Materials and sample preparation

Matrix	Sample preparation
PPb	Quenched
PPb	Isothermal crystallisation 125°C, 1min
PPb	Isothermal crystallisation 125°C, 5min
PPb	Isothermal crystallisation 130°C, 60min
PPa	Constant cooling rate 10°C/min
PPb	Constant cooling rate 10°C/min

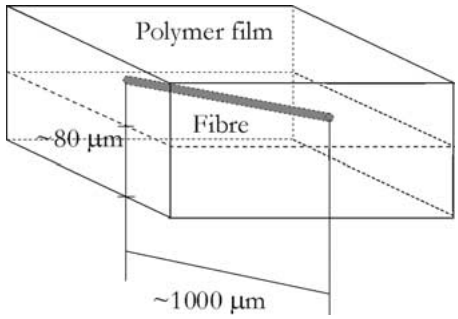

Figure 1 Manufacturing of single fibre composites utilising the thermal stage.

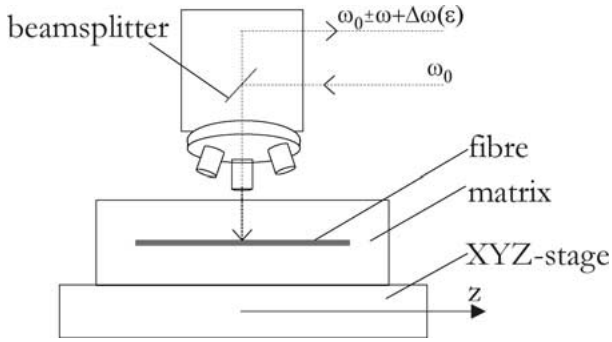

Figure 2 Raman spectrum acquisition using Raman microprobe (ω_0: laser frequency, ω: Raman frequency, $\Delta\omega(\varepsilon)$: Raman band shift with strain).

the exposed surface was determined using a thermocouple and read-out values were corrected accordingly. The composites were cooled at constant cooling rates or isothermally crystallised. Details of the sample preparation are given in Table I.

2.2. Raman spectroscopy

Thermal stresses were measured using Raman spectroscopy. The sample was placed on a motorised and computer controlled XYZ-stage and the laser was focused confocally in the fibre through a ×50 objective to obtain a laser spot of approximately 2 μm in diameter. This enables Raman spectra to be recorded at different points on the fibre and thus to determine the thermal stress distribution along the fibre (Fig. 2).

The 2660 cm^{-1} second-order peak was used to determine stress in the fibre. The Raman band shift with compressive strain for this band has previously been determined to $-19.98\ cm^{-1}/\%$ [26]. Axial stress in the fibre was calculated as $\sigma = E^f \varepsilon$ where $E^f = 350$ GPa is the longitudinal Young's modulus of the fibre.

2.3. Data analysis

Experimental data were fitted to a partial elastic shear-lag distribution

$$\sigma_z^f = \underbrace{-\frac{2\tau_I z'}{r^f}}_{in-elastic} + \underbrace{\left(E_f\varepsilon^\infty + -\frac{2\tau_I z'}{r^f}\right)\left(1-\frac{\cosh(nL+n|z'-z|)}{\cosh(nL)}\right)}_{elastic} \quad (1)$$

The in-elastic stress transfer may either be frictional slip or yielding. The parameters of Equation 1 are

$$n = \frac{1}{r^f}\sqrt{\frac{2E_m}{E_f(1+\nu_m)\ln\left(r_m^2/r_f^2\right)}}$$

E^f = fibre modulus, r^f = fibre radius, r^m = matrix radius, ε^∞ = farfield thermal strain, z' inelastic stress transfer, f = fibre volu and L = fibre length.

Equation 1 can be written in a simple form

$$\sigma_z^f = -\frac{2\tau_I z'}{r^f} + \left(C_1 + -\frac{2\tau_I z'}{r^f}\right) \times \left(1-\frac{\cosh(C_2 - C_3|z'-z|)}{\cosh(C_2)}\right) \quad (2)$$

Thus the shear-lag solution can be fitted to experimental results by determining the constants τ_f, z', C_1, C_2, C_3 through a least squares analysis.

From the experimental fit the shear stress was calculated by differentiation as

$$\tau_{rz}^f = \frac{1}{2} r^f \frac{d\sigma_z^f}{dz} \quad (3)$$

3. Results and discussion

Fig. 3 shows the microstructure of samples that have been quenched from melt or isothermal crystallised. In the isothermal crystallised sample a transcrystalline interlayer has been formed. Fig. 4 shows the thermal stress distribution for these two samples. The stress distribution indicates an in-elastic stress transfer for $z < 350$ μm and elastic stress transfer for $z > 350$ μm. The interfacial shear stress in the slip zone was found to be 5.31 MPa for the transcrystalline sample and 3.66 MPa for the quenched sample. These values are much lower than the shear yield limit of PP (≈15 MPa) indicating that the stress transfer in the in-elastic zone is frictional slip. This increase in stress transfer in the presence of a transcrystalline interlayer may either be related to the increased radial pressure or an increase in the "frictional" coefficient. Brady and Porter /20/ have shown that the adsorption rather than the heterogeneous nucleation explains the increase in adhesion. Adsorption is primarily governed by MW and melt-time/temperature. These parameters were the same for the two systems of Fig. 4. Thus the increase in interfacial adhesion in the case of transcrystallisation is probably due to an increased radial stress at the interface.

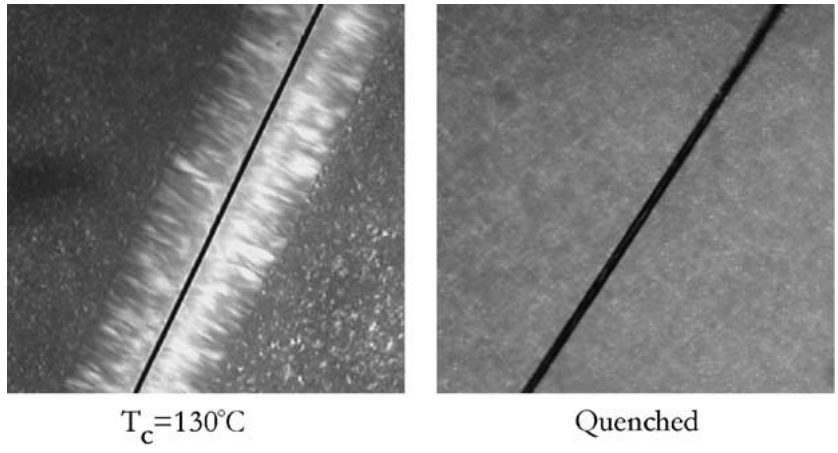

Figure 3 Microstructure of sample isothermal crystallised at 130°C followed by quenching and sample quenched directly from the melt.

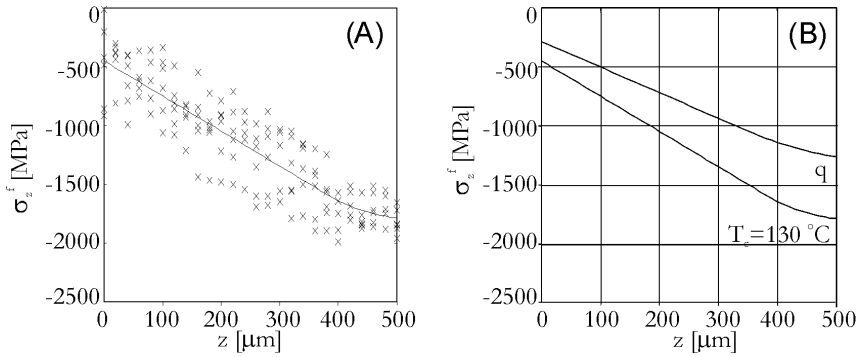

Figure 4 Thermal stress distribution in fibre: (A) Isothermal crystallised sample and (B) Compared with quenched sample (data regressions).

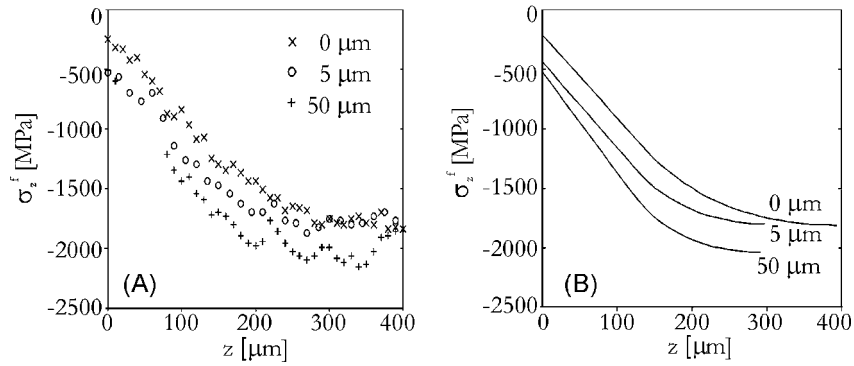

Figure 5 Influence of thickness of transcrystalline interlayer: (A) Experimental data and (B) Data regression (numbers on graphs indicate approximate crystallisation time/interlayer thickness.

To further investigate the transcrystalline phenomenon samples were prepared with transcrystalline interlayers of different thicknesses (different crystallisation times) (Fig. 5). The increased stress transfer efficiency with increased thickness of the transcrystalline interlayer supports the conclusion that the influence of the transcrystalline interlayer is due to increased radial stress rather than an adhesion phenomena. An increase in radial compressive stress may either be due to different properties of the transcrystalline interlayer as compared to the bulk morphology. As spherulites preferentially grow radially to the fibre, the transcrystalline interlayer must be anisotropic due to the mechanical and thermal anisotropy of the crystal unit cell [27, 28]. However the increase in radial stresses may also be due to the different thermal history to which the samples have been subjected. The isothermally crystallised sample solidifies readily upon quenching from the crystallisation temperature, whereas the quenched sample will solidify at a significantly lower temperature due to the influence of cooling rate on crystallisation. Thus the isothermally crystallised sample will have a higher stress free temperature, which will affect the residual normal stress at the interface.

Fig. 6 shows the microstructure of two samples with different matrices, PPa and PPb, cooled at 10°C/min. In the PPa matrix system spherulites are not heterogeneously nucleated. As these samples have been subjected to the same cooling rate, the morphology only differs by the presence of the transcrystalline interlayer in the PPb matrix composites, whereas the bulk morphologies are similar. Fig. 7 shows the thermal stress in

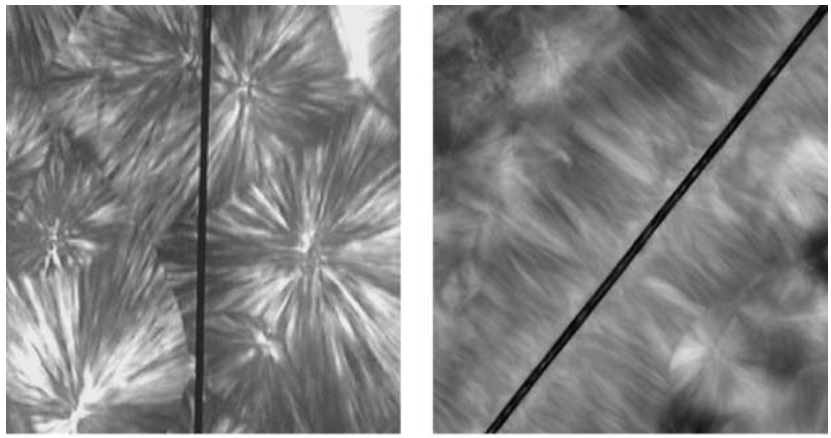

Figure 6 Morphology of HM-PPa (spherulitic) and HM-PPb (transcrystalline) cooled at 10°C/min.

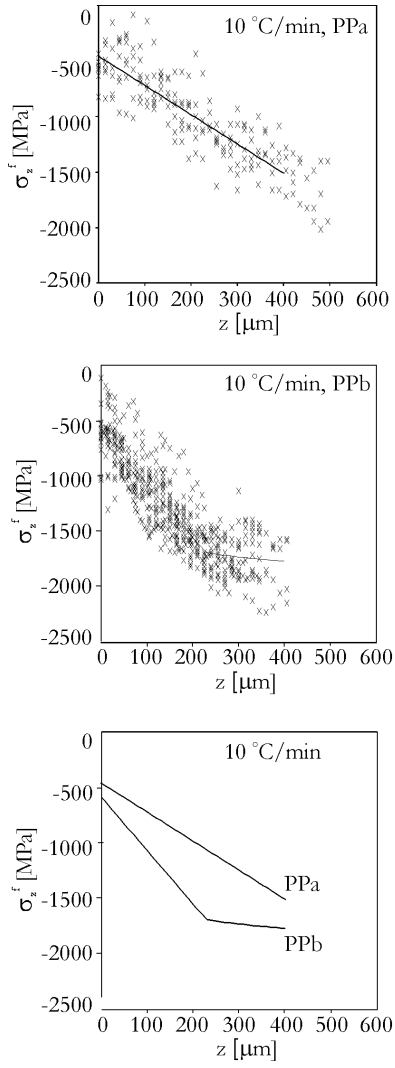

Figure 7 Stress distribution in PPa and PPb matrix composites cooled at 10°C/min, (A) PPa, (B) PPb, and (C) Comparison of data regressions.

the fibre of PPa and PPb systems cooled at 10°C/min. Thus the increase in stress transfer efficiency must primarily be due to the presence of an anisotropic transcrystalline interlayer.

4. Conclusions

Thermal stresses have been measured in polypropylene matrix composites using micro Raman spectroscopy. The existence of a transcrystalline interlayer increases the residual shear stress by causing a more efficient stress transfer. The experimental results, as well as previous studies, conclude that stress transfer in polypropylene matrix composites is governed by friction. In this case stress transfer is governed by radial stress and coefficient of friction. The explanation for the increase in interfacial shear stress in the presence of a transcrystalline matrix was explained by increase in radial stress as result of the anisotropic nature of the transcrystalline interlayer.

References

1. M. J. FOLKES, "Polypropylene, Structure, Blends and Composites: Composites" (Chapman & Hall, London, 1995) p. 340.
2. E. J. H CHEN and B. S. HSIAO, *Polym. Eng. Sci.* **32** (1992) 280.
3. Y. LEE and R. S. PORTER, *ibid.* **26** (1986) 633.
4. M. AVELLA, G. D. VOLPE, E. MARTUSCELLI and M. RAIMO, *ibid.* **32** (1992) 376.
5. D. CAMPBELL and M. M. QAYYUM, *J. Polym. Sci. Polym. Phys. Ed.* **18** (1980) 84.
6. W. S. CARVALHO and E. S. BRETAS, *Eur. Polym. J.* **26** (1990) 817.
7. J. M. FELIX and P. GATENHOLM, *J. Mater. Sci.* **29** (1994) 3043.
8. M. J. FOLKES and W. K. WONG, *Polymer* **28** (1987) 1309.
9. S. INCARDONA, H. D. WAGNER, A. H. GILBERT and G. MAROM, *Comp. Sci. Techn.* **47** (1993) 43.
10. N. KLEIN, G. MAROM, A. PEGORETTI and C. MIGLIARISI, *Composites* **26** (1995) 707.
11. N. KLEIN, G. MAROM and E. WACHTEL, *Polymer* **37** (1996) 5493.
12. L. REBENFELD, G. P. DESIO and J. C. WU, *Appl. Polym. Sci.* **42** (1991) 801.
13. T. STERN, G. MAROM and E. WACHTEL, *Composites* **28 A** (1997) 437.
14. T. STERN, A. TEISHEV and G. MAROM, *Comp. Sci. Techn.* **57** (1997) 1009.
15. J. L. THOMASSON and A. A. VAN ROOYEN, *J. Mater. Sci.* **27** (1992) 889.
16. *Idem., ibid.* **27** (1992) 897.
17. A. TREGUB, H. HAREL and G. MAROM, *J. Mater. Sci. Letters.* **13** (1994) 329.
18. C. WANG and L. M. HWANG, *J. Polym. Sci. Polym. Phys. Ed.* **34** (1996) 47.
19. R. L. BRADY and R. S. PORTER, *J. App. Polym. Sci.* **39** (1990) 1873.
20. M. HEPPENSTALL-BUTLER and R. J. YOUNG, *J. Mater. Sci. Letters* **14** (1995) 1638.
21. M. HEPPENSTALL-BUTLER, D. J. BANNISTER and R. J. YOUNG, *Composites* **27 A** (1996) 833.

22. A. S. NIELSEN and R. PYRZ, *Composite Interfaces* **6** (1999) 467.
23. B. PUKANSKY in "Polypropylene: Structure Blends and Composites: Composites" edited by J. Karger-Kocsis (Chapmann and Hall, London, 1995).
24. J. J. ELMENDORP and G. E. SCHOOLENBERG, in "Polypropylene: Structure Blends and Composites: Composites" edited by J. Karger-Kocsis (Chapmann and Hall, London 1995) p. 228.
25. B. Z. JANG, in "Polypropylene: Structure Blends and Composites: Composites" edited by J. Karger-Kocsis (Chapmann and Hall. London, 1995) p. 316.
26. A. S NIELSEN and R. PYRZ, *Polym. and Polym. Comp.* **5** (1997) 245.
27. J. R. ISASI, R. G. ALAMO and L. MANDELKERN, *J. Polym. Sci. Phys. Ed.* **35** (1997) 2945.
28. K. TASHIRO, M. KOBAYASHI and H. TADOKORO, *Polym. Journal.* **24** (1992) 899.

Received 9 August 2001
and accepted 24 September 2002